DOI 10.1007/s10946-022-10082-x
Journal of Russian Laser Research, Volume 43, Number 5, September, 2022

FINITE ELEMENT THERMAL ANALYSIS OF OPTICAL ELEMENTS IN A LASER INCOHERENT SPACE BEAM COMBINER

Xiao Tian,[1,2,3] Yang Bai,[1,3*] Ben Li,[1,3] Facheng Jin,[2] and Lidong Yu[1,3]

[1] *Institute of Photonics and Photon Technology, Northwest University Xi'an 710127, Shaanxi, China*

[2] *School of Science, Xi'an Aeronautical University Xi'an 710077, Shaanxi, China*

[3] *Shaanxi Engineering Technology Research Center for Solid State Lasers and Application Xi'an 710127, Shaanxi, China*

*Corresponding author e-mail: by@nwu.edu.cn

Abstract

We report an 11 kW laser incoherent space beam combiner with circular spot, which uses 19 semiconductor laser beams of about 972 nm. Based on the established multi-beam laser volumetric heat source model, the thermal–mechanical performance of all optical elements in the beam combiner, including temperature field, thermal deformation, and thermal stress, is analyzed, using the finite element method (FEM). The high accuracy of FEM model is verified based on the high coincidence between the experimentally measured and simulated temperature values of the window element. After a continuous operation of 1,800 s, the maximum beam combining power of the circular combining laser beam reaches 11 kW (measurement uncertainty ±3%). Results of theoretical simulations and experimental measurements show that the beam combiner has good safety and stability under the long-time irradiation beyond the 11 kW high-power laser. Our research has a reference value for an effective evaluation of the working performance of ultra-high-power laser systems.

Keywords: laser incoherent space beam combining, 11 kW, volume heat source, finite element thermal analysis.

1. Introduction

High-power laser source is widely applied in a vast number of fields, such as industry, aerospace, and military equipment [1–3]. Incoherent space laser beam combination is one of the effective methods to mitigate the transmission risk of high-power laser in a single fiber and achieve high-energy laser output [4–6]. It is characterized by the high-output power capability, compactness, and robust design. The laser power of more than 10 kW can be provided now. For high-power combiner, a large number of optical elements made of fused silica material is used to realize the collimation and beam combination of the multi-beam laser. Fused silica is the preferred material for the manufacture of optical components in the combiner due to its low UV absorption, resistance to laser damage, and good thermal and mechanical stabilities. However, the heat accumulation generated by long-time high-power laser-beam irradiation is likely to produce serious thermal effect in the optical components [7–9]. With increase in the irradiation

Manuscript submitted by the authors in English on April 29, 2022.

laser power, the temperature of the optics increases, leading to more severe thermal deformation of optical elements, which will seriously affect the safety and reliability of the combiner. The performance degradation or failure of the combiner is unacceptable. However, the deformation and fracturing of these elements always happen during their operation, especially, in the case that the mechanical structure of the combiner is shielded, the thermal–mechanical properties of these optical elements are difficult to be directly detected and evaluated, using general experimental methods. While in the meantime, a number of numerical models established, using the finite element method (FEM), has been developed to study the thermal–mechanical process of used silica affected by high-power lasers [10–12]. At present, most of the researches simplified the irradiation effect of laser beam on optical elements as the surface heat source, ignoring the absorption of laser energy inside the optics [8, 13]. The volume absorption of the transmitted laser beam by the optical-element material itself is one of the main factors affecting the thermal–mechanical properties of the optical elements, and therefore, it is highly necessary to consider the heat absorption inside the material. Although the study [14] treated the laser irradiation on the material as a bulk heat source, and the heat source was originated from a single laser beam, there are few reports on the thermal–mechanical finite element analysis of multi-beam ultra-high power transmission optics, using the laser beam as a volumetric heat source, which is critical for the performance evaluation of the high-power combiner irradiated by the laser for a long time.

In the paper, we investigate the coupled thermal–mechanical performance of optical elements in an 11 kW 19×1 laser incoherent space beam combiner with circular spot, in view of FEM. In the meantime, a multi-beam laser volumetric heat source model is established based on the overall heat source distribution of 19 laser beams, synchronously transmitted through optical elements in the beam collimation units (BCU) and the space beam combining unit (SBCU). The distribution and evolution of temperature field, thermal deformation and stress of all optical elements in the beam combiner are discussed. The research can provide a reference for the safety and reliability evaluation of the ultra-high-power laser space beam combining system.

2. Design of Beam Combiner with Circular Spot

The beam combiner based on the incoherent space beam combining principle is shown in Fig. 1 a, with coaxial arrangement of "center + inner & outer concentric circles" [5]. 19 fiber-coupled near-infrared diode lasers have the wavelength of about 972 nm and output power of more than 600 W per laser beam. The core diameter of each transmission fiber is 400 μm, with a numerical aperture (N.A.) of 0.22. The beam combiner contains 19 BCUs for collimating each divergent laser beam output from the transmission fiber and 1 SBCU for combining 19 collimated beams in parallel with each other. Each BCU contains a lens array composed of lenses m_1, m_2, and m_3. After passing through BCU, the laser beam output is transformed by the transmission fiber into a collimated laser beam with a spot radius of 3.5 mm and a divergence angle of 15 mrad. The center distance d between any two parallel collimated laser beams is determined to be 15 mm to ensure that the beam combiner has the smallest radial dimension and necessary structural strength [5].

According to the project requirements, after the focusing and beam combining operation of SBCU, 19 collimated laser beams are shaped into a single beam with a circular spot in the diameter of 15 mm within a combined beam length of 250 mm. The parameters, including quantity, diameter, curvature radius of the light-transmitting surface, and adjacent spacing of each elements in SBCU, are optimized, using the ray tracing method to satisfy the above technical requirements. In Fig. 1 b and c, we show the

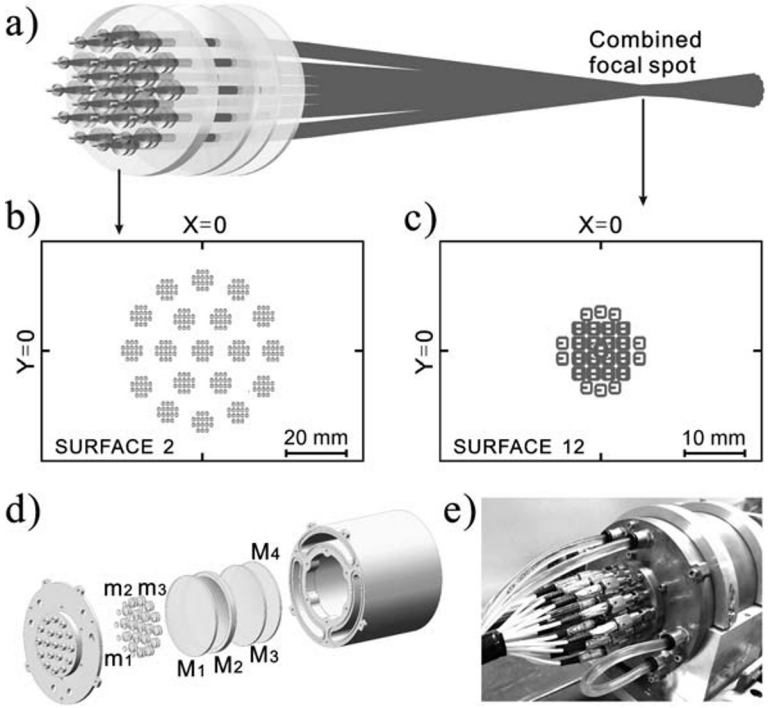

Fig. 1. Schematic design of beam combiner with a circular spot (a), ray-tracing lattice cross-section of 19 laser beams on first incident surface of SBCU (b), ray-tracing lattice cross-section at the position of combined focal spot (c), overall axial split type of 3D design drawing for beam combiner (d), and photo of beam combiner (e).

ray tracing distributions of the laser spot on the incident surface of the first beam-combining lens M_1 and the beam-combining focal spot surface of SBCU, respectively. The optimized SBCU with a combined focal length of 1,000 mm is composed of three spherical lenses, i.e., M_1, M_2, M_3, and a plane window M_4. In the direction from the end face of the fiber to M_4, the distances between adjacent elements are 5.4, 9.4, 4.0, 21.5, 12.1, 30.4, and 21.6 mm, respectively. The parameters of all optical elements are summarized in Table 1. All optical elements are coated with antireflection coating ($R < 0.4\%$) at the 972 nm wavelength.

Table 1. Parameters of Optical Elements in Beam Combiner in [mm].

Element	Radius		Thickness	Diameter
	Incident surface	Exit surface		
m_1	−72	+5	2	7
m_2	+20	−12	2	10
m_3	+30	+15	4	10
M_1	∞	+400	9	85
M_2	−156	+160	10	85
M_3	∞	+224	13	85
M_4	∞	∞	3	85

As shown in Fig. 1 d and e, a cylindrical space with a diameter of 85 mm is formed by the 19 BCUs and 1 SBCU as a whole, which is surrounded by annular cooling water at 20°C with a thickness of 10 mm. In the environment with a stable temperature of 20°C, the heat generated by all optical elements absorbing laser energy will be quickly removed. Therefore, the influence of the reflection part and scattering part of the 19 laser beams on the safety and stability of the beam combiner can be ignored. The outer diameter and length of the beam combiner were designed to be 125 and 145 mm, respectively. According to the parameters of 19 BCUs and SBCU, the beam combiner was made of H85 brass with high thermal conductivity and good mechanical properties.

3. Multi-Beam Laser Volumetric Heat Source Model

We establish the model to study the thermal–mechanical coupled process of the combined laser beam with the power of more than 11 kW irradiating the fused silica optical elements in the combiner. For the control equations [15], 3D transient heat conduction equation and the mechanical equilibrium equation are given as follows:

$$\rho C_p(T)\frac{\partial T}{\partial t} + \nabla \cdot [-K(T)\nabla T] = Q, \tag{1}$$

$$\rho\frac{\partial^2 u}{\partial t^2} = \nabla\sigma + F_v, \tag{2}$$

where ρ refers to the density, C_p stands for the heat capacity, K represents the thermal conductivity, Q denotes the heat source originated from the laser energy absorption, and T is the temperature. In addition, σ refers to the stress tensor, F_v stands for the unit body force, and u represents the displacement.

For the beam combiner, the initial temperature $T(t = 0) = T_0$. An optical element is in contact with the copper sleeve, and there is a gap between the surface of the element edge and that of the copper sleeve filled with air. The light passing the surface contacts the air directly. Therefore, it is deemed that heat convection exists on all surfaces of the optics. The condition is applicable to the finite element analysis for all optical elements, and thermal radiation is taken into account for the accurate analysis. Therefore, the thermal boundary condition is expressed as

$$-K\frac{\partial T}{\partial n} = h(T - T_0) + \sigma\varepsilon(T^4 - T_0^4), \tag{3}$$

where n refers to the value of the normal outward vector of the geometric model surface, and h stands for the heat transfer coefficient. The thermal radiation coefficient for the fused silica material is $\varepsilon = 0.8$.

For the structural constraint, a fixed boundary condition is applied to the periphery of the elements fixed to the copper sleeve based on the engineering structure of the combiner, thereby preventing the free thermal expansion. Therefore, the corresponding thermal displacement of the fixed surface $u(t)$ is equal to zero, and what inside the element is the sum of the thermal deformation and mechanical boundary condition.

The heat source term Q is originated from the energy deposition in the depth of the material, which works as a volumetric heat source to produce thermal effect on optical elements. The attenuation of the laser beam in the material with the depth from the surface and the absorption coefficient are taken into account. Assuming that the Gaussian laser beam propagates along the z axis, the volume heat source Q reads

$$Q = \alpha(1 - R)\frac{2P}{\pi\omega^2}\exp\left(-2\frac{x^2 + y^2}{\omega^2}\right)\exp(-\alpha z), \tag{4}$$

where P refers to the laser power irradiating the material, ω stands for the $1/e$ beam radius, R represents the Fresnel reflection coefficient, and α is the absorption coefficient of material.

The heat source expressed in Eq. (4) is used to analyze the thermal–mechanical property of optical elements in BCU, which are irradiated by a single laser beam of 600 W. Different from the heat source expressed in Eq. (4), 19 laser beams pass through the combining elements simultaneously for SBCU. A total volume heat source for the space incoherent beam combination, which is obtained after the

modification of Eq. (4), using the space distribution parameters of 19 laser spots, is

$$Q = \sum_{i}^{19} Q_i = \alpha \frac{2(1-R)P}{\pi\omega^2} \exp\left\{-2\left[\frac{(x+\Delta x_i)^2}{\omega^2} + \frac{(y+\Delta y_i)^2}{\omega^2}\right]\right\} \exp(-\alpha z), \quad (5)$$

where Q_i refers to the volume heat source generated by the first laser beam, and $x+\Delta x_i$ and $y+\Delta y_i$ represent the position, where each laser beam reaches the incident faces of the elements M_1, M_2, M_3, and M_4 in SBCU. Taking ($x = 0$, $y = 0$) as the coordinate origin, Δx_i and Δy_i indicate the offset from the combined beam center on each incident face of the elements in SBCU.

As shown in Fig. 2, 19 laser spots are arranged in the inner and the outer concentric circles, and L_i and $2L_i$ denote the radii of the inner and outer circles, respectively. For the spot located at the center, the coordinate position is set as $x = 0$, $y = 0$; while for the positions of 6 spots on the inner circle and 12 spots on the outer circle, the flare angle of the arc corresponding to the adjacent light spot is $\theta_1 = \pi/3$ and $\theta_2 = \pi/6$, respectively. Using the ray tracing method, we obtain the actual parameters of 19 laser spot radii and the arrangement circle sizes in each element of SBCU; see Table 2. The corresponding positions of the 19 laser spots on each combining elements are then calculated and used for the total volume heat source expressed by Eq. (5).

Taking the laser heat sources of the optical elements in BCU and in SBCU, respectively, expressed by Eqs. (4) and (5) as the thermal load, the transient temperature of the elements m_1 to m_3 and M_1 to M_4 can be obtained with FEM by solving Eqs. (1)–(3) combined with the boundary conditions. The properties of fused silica are shown in Table 3 [14–16]. Further, the coupled simulation of the stress fields can be carried out based on the temperature field results.

In general, the value of air heat transfer coefficient h varies between 5 and 30 W/(m^2·K). To analyze the thermal–mechanical characteristics of all optical elements in the combiner more exactly, a more accurate h value is needed. In this paper, the temperature of the exit surface of the window protective element M_4 in the combiner was measured

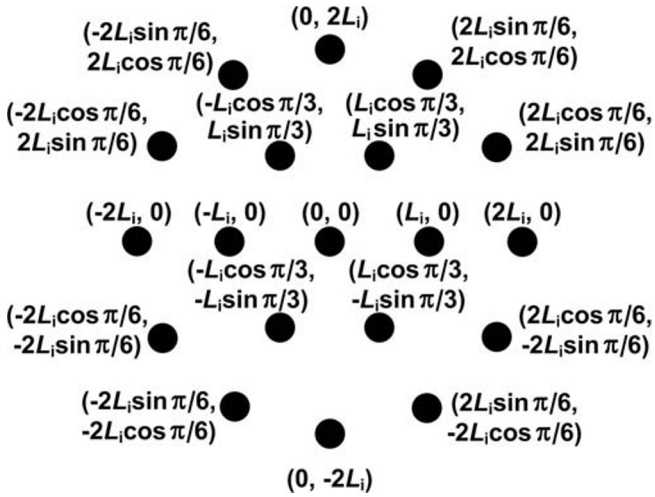

Fig. 2. Center coordinates (x, y) of 19 laser spots on the incident surface of each element in SBCU.

Table 2. Laser Spot Size and the Arranged Circle on Each Combining Elements in [mm].

Parameter	M_1	M_2	M_3	M_4
Spot radius	3.5	3.2	2.1	1.5
L_i	15.0	13.9	12.8	11.3

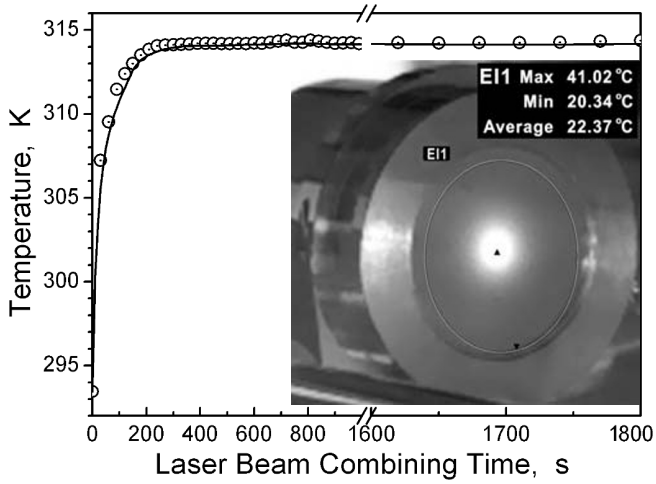

Fig. 3. Comparison of the experimental (⊙) and the simulated (the solid curve) temperature for h = 9.5 W/(m^2 · K). The inset is the photo of M_4 thermal image at 1,800 s.

experimentally at different times, using FLIR-T5590 thermal imager. Considering the energy loss, the actual power was about 584 W, when the laser with an initial power of 600 W reached M_4. The optimum value of h was finally determined to be 9.5 $W/(m^2 \cdot K)$ by linear fitting to the experimental measurements based on Eqs. (1)–(4) and the properties presented in Table 3; see Fig. 3.

Table 3. Properties of Fused Silica in the Calculations.

Parameter	Value	Unit
Density	2202	kg/m^3
Heat capacity	$35.94 + 3.37\,T - 0.004\,T^2 + 2.58 \cdot 10^{-6}\,T^3$	$J/(kg \cdot K)$
Heat conductivity	$0.98 + 1.12 \cdot 10^{-3}\,T$	$W/(m \cdot K)$
Heat expansion	$5.18 \cdot 10^{-7}$	1/K
Thermal radiation coefficient	0.8	
Poisson ratio	0.17	
Absorption coefficient at 972 nm	0.105	1/m
Young's modulus	$7.56 \cdot 10^{10}$	Pa
Bulk modulus	$3.87 \cdot 10^{10}$	Pa
Shear modulus	$3.19 \cdot 10^{10}$	Pa

4. Thermal–Mechanical Properties of Optical Elements

It is worth noting that the elements in SBCU are irradiated simultaneously by 19 laser beams with a total power of more than 11 kW. Therefore, the primary task to evaluate whether the beam combiner can work safely and reliably for a long time is to simulate and analyze the temperature field and thermal stress distribution law of the elements in SBCU, in view of FEM. The objective is to judge whether the maximum temperature, thermal stress, and thermal deformation variable of each element exceed the softening temperature, yield stress, and allowable deformation variable of fused silica glass, correspondingly.

4.1. Temperature Field

There are 19 laser beams propagating in the axial direction (z axis). The elements in SBCU are irradiated by the 19 laser beams for the duration ranging from 0 to 1,800 s, and the power after passing the single BCU is about 589 W. The absorption loss of the laser power is considered to calculate the actual temperature value of each element. The temperature distributions of the elements M_1–M_4 are shown in Figs. 4 a–d.

It is consistent with the laser spot distributions on the surfaces of the corresponding elements. The heat accumulation generated by the laser heat source inside the element causes the maximum temperature of each element to be at itself center. In the beam combining direction, the overall irradiation volume of the 19 laser beams is gradually compressed due to the beam combining focus, and the total laser power volume density is continuously and accordingly increased. Consequently, the optical elements with larger central thickness absorb laser energy more seriously, while those with smaller edge thickness has lower radial thermal conductivity. Therefore, a maximum temperature of 382 K on the exit surface of the lens

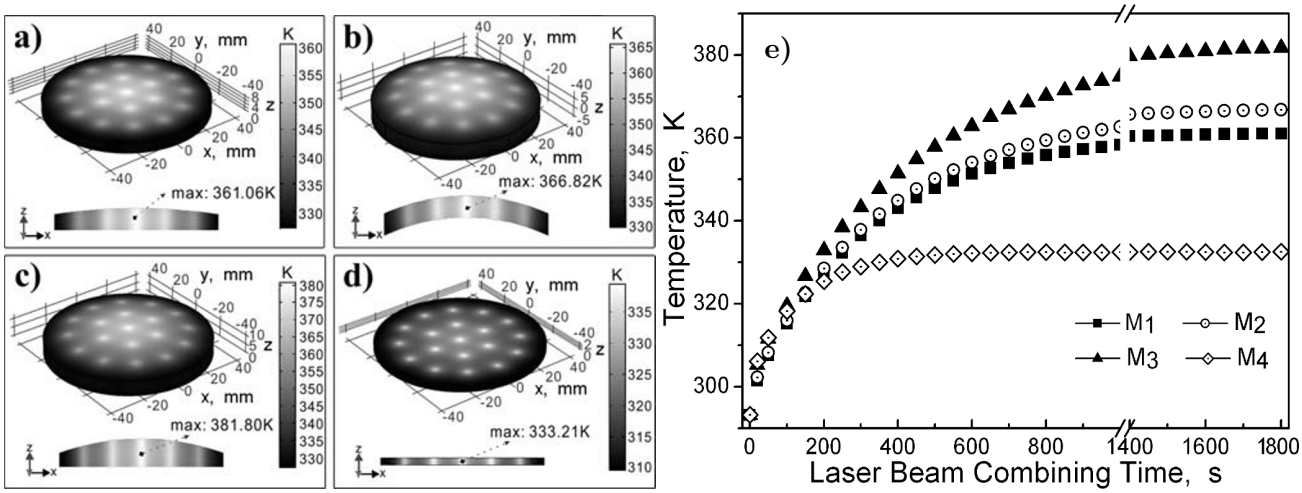

Fig. 4. Temperature distributions in M_1 (a), M_2 (b), M_3 (c), and M_4 (d) irradiated by 11 kW laser for 30 min, and the maximum temperature of 4 elements in SBCU as a function of laser beam combining time (e).

M_3 is the largest, which is followed by those of M_2, M_1, and M_4, and much lower than the softening point of UV fused silica (1,900 K) [17]. The variation of the maximum temperature of the elements M_1–M_4 with the beam combining time is shown in Fig. 4 e. Each optical element reached thermal equilibrium after nearly 1,400 s.

4.2. Thermal Deformation and Thermal Stress

We use the temperature gradient originated from the combined high-power irradiation as the thermal load to analyze the deformation and stress of the elements in SBCU. First, the distributions of the total thermal displacement are shown in Fig. 5 a–d. The results show that the distribution of the thermal displacement on each element is consistent with its temperature distribution, and the region without

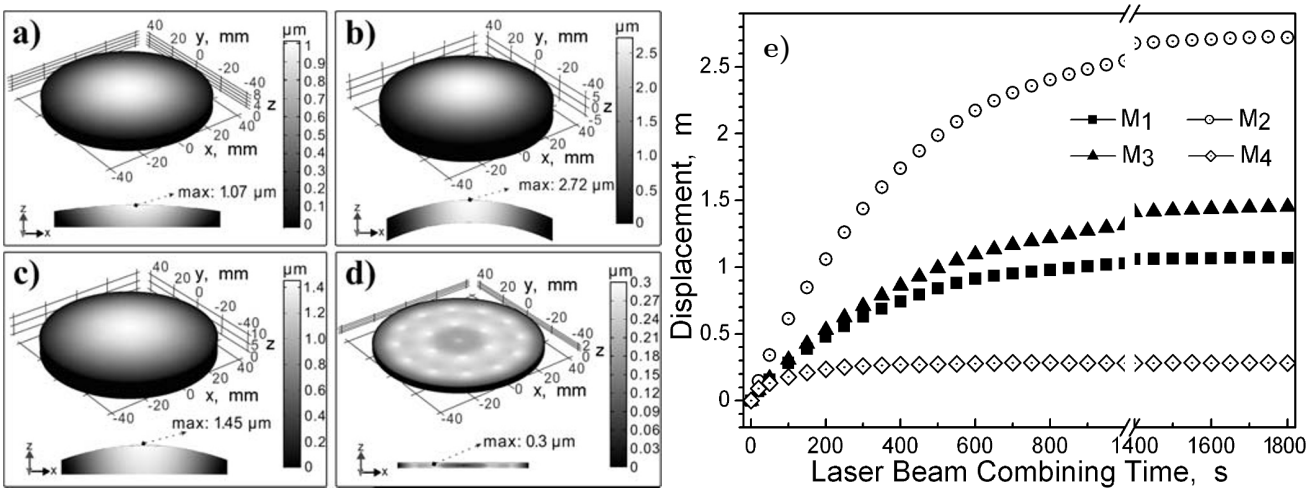

Fig. 5. Thermal deformation distribution in M_1 (a), M_2 (b), M_3 (c), and M_4 (d), and maximum displacement of 4 elements as a function of laser beam combining time (e).

displacement is located at the edge of the element, which is in perfect agreement with the structural constraint $u = 0$. Since the edge thickness of M_2 is greater than its central thickness, and the center of mass is not inside its body, the volume shrinkage caused by cooling at the edge of the element body is greater than that of other elements. With the small difference of the maximum temperature in the center, the maximum distortion of lens M_2 is 2.7 μm, which is the largest among the 4 elements in SBCU followed by those of M_3, M_1, and M_4. Moreover, the displacement evolution of M_1–M_4 is shown in Fig. 5 e and becomes stable after 1,400 s.

To evaluate the influence of thermal deformation on the laser beam combining quality, we obtain the thermal deformation values for the curvature radius of the optical element surfaces, using Zernike polynomial fitting method [18], and express as aperture number Ψ [19] as follows:

$$\Psi = \left(\frac{D_i}{2\,R_a}\right)^2 \cdot \frac{\Delta R_a}{\lambda}, \tag{6}$$

where D_i and R_a refer to the diameter and the curvature radius of the light passing surface before laser irradiation, respectively, ΔR_a stands for the thermal deformation of the curvature radius of the light-passing surface after laser irradiation, and λ is 972 nm.

As shown in Table 4, the aperture number Ψ corresponding to a maximum deformation of 2.72 μm is only 0.07, which is much smaller than the machining tolerance requirements of elements with an aperture number of 1. Therefore, it is verified that, under the long-term irradiation of 11 kW laser beams, the optical elements in SBCU have no impact on the beam combining imaging quality due to excessive thermal deformation.

Table 4. Thermal–Mechanical Properties of Optical Elements in the Beam Combiner.

Element	$\Delta T_{\max}$, K	$D_{\max}$, μm	$F_{\max}$, MPa	Ψ
m_1	10	0.2	14.0	0.01
m_2	9	0.1	3.4	0.01
m_3	8	0.1	7.7	0.01
M_1	65	1.1	5.3	0.03
M_2	70	2.7	11.5	0.07
M_3	85	1.5	10.1	0.04
M_4	43	0.3	1.5	0.01

After that, we analyzed the distributions of von Mises stress of the elements in SBCU and the variation of the stress with the irradiation time; see Fig. 6. According to the theory of plastic mechanics, the thermal stress in an element is transferred to the fixed constraint position of its edge. The incident surfaces of the lenses M_1–M_3 are convex, and the thermal stresses in them are rapidly transferred to the edges of their bodies. A large amount of stress accumulation will be formed at their edges, and the maximum thermal stresses result in a circular symmetrical distribution along the edges. While M_4 is a plane window, and the structural characteristics of its center thickness and edge thickness are the same. Therefore, the transmission speed of thermal stress to its edge is slow, which results in the stress accumulation and maximum thermal stress formation in the center of the element body. In addition, the relationship between the maximum stress of the elements is related to the corresponding thermal deformation. Therefore, a thermal stress of 11.5 MPa from lens M_2 is the largest, which is followed by those of M_3, M_1, and M_4. The stresses remain unchanged after 1,400 s, and a maximum stress of 11.5 MPa is significantly less than the yield stress of 50 MPa of fused silica [20].

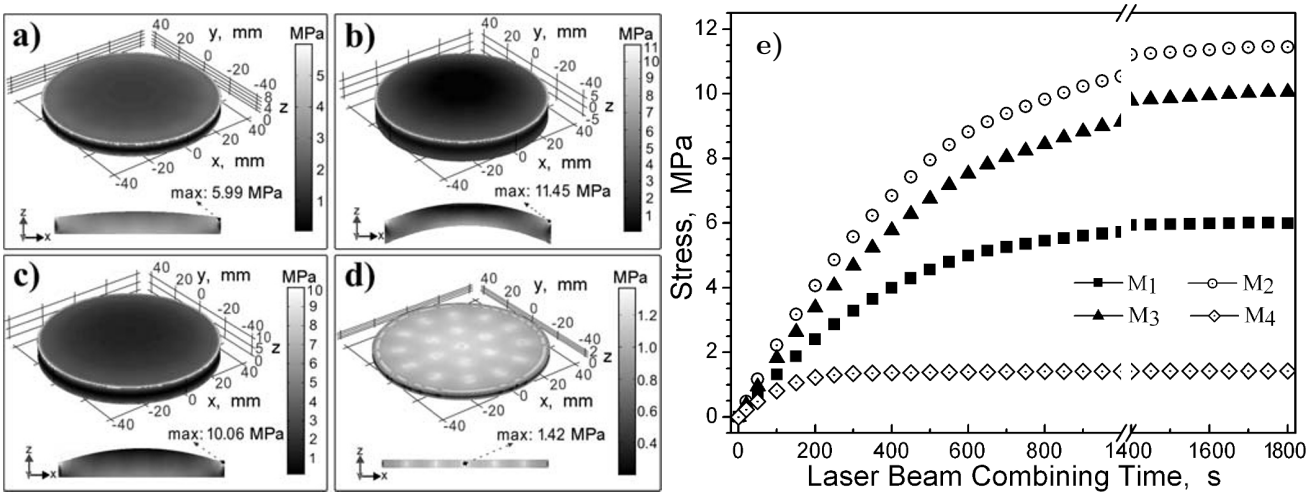

Fig. 6. Thermal stress distributions in M_1 (a), M_2 (b), M_3 (c), and M_4 (d), and the maximum stress of 4 elements as a function of laser beam combining time (e).

4.3. Thermal–Mechanical Properties of Optical Elements in BCU

When a single laser beam with a power of 600 W is transmitted, since the structural parameters of the 19 BCUs are the same, in this paper, only the thermal–mechanical properties of the three lenses in a BCU are analyzed, using the volume heat source, as expressed in Eq. (4). The diameters of single-beam on lenses M_1, M_2, and M_3 are 1.5, 2.6, and 3.1 mm, respectively. The related thermal–mechanical parameters at a time node of 1,800 s are shown in Table 4. One can see from the results that the maximum temperature difference $\Delta T_{\max}$, the maximum thermal deformation $\Delta D_{\max}$, and the maximum thermal stress $F_{\max}$ of all optical elements in BCU are all smaller than the corresponding data of the optical elements in SBCU.

5. Comparison with Experimental Measurement

The thermal–mechanical simulation parameters listed in Table 4 provide a theoretical basis for verifying the good safety and reliability of the combiner during long-term operation. Based on this, the long-term operational reliability of the beam combiner is studied. As shown in Fig. 7, when the maximum current drive of a single semiconductor laser is 38 A, and 19 sets of 972 nm semiconductor lasers work simultaneously for 1,800 s, the laser beam combining power is as high as 11 kW, as measured by a power meter with a calibration uncertainty of ±3% at 972 nm.

In the meantime, to verify the accuracy and reliability of our model, we compare the simulated

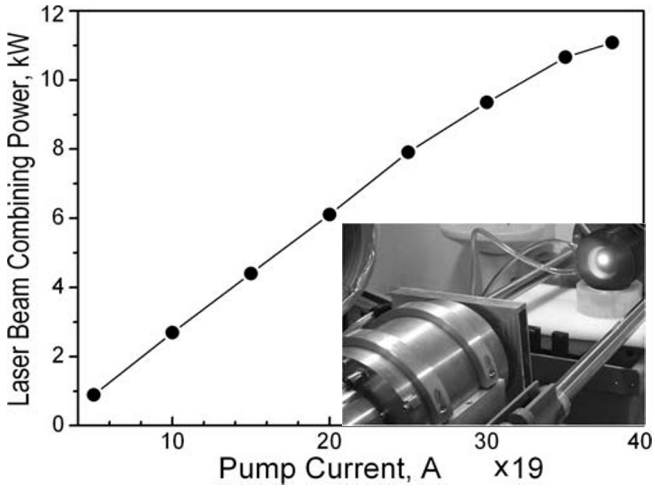

Fig. 7. The 19 beam combiner output power versus the semiconductor-laser pump current. The inset is a photo of the combiner at high output beam power.

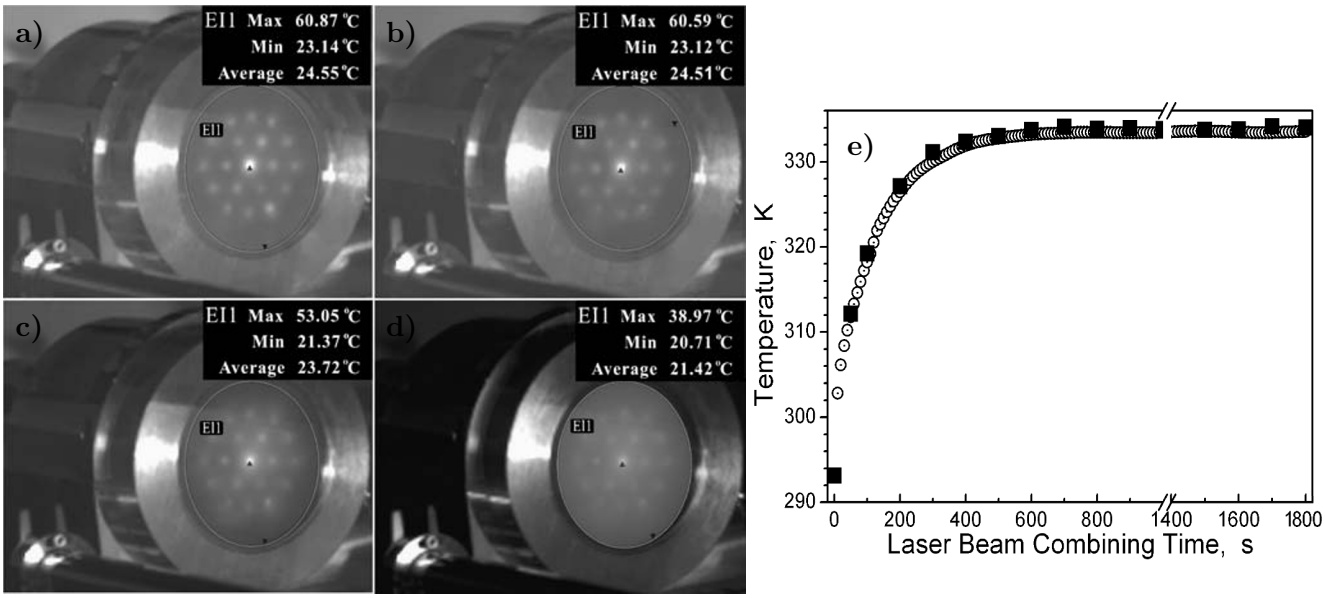

Fig. 8. Temperature photos of the exit surface of M_4 during 11 kW laser beam combining period at 50 s (a), 200 s (b), 1,400 s (c), and 1,800 s (d), using a thermal imager based on the model above established, along with the temperature measured in the experiment (■) and the simulated temperature during a 11 kW laser beam combining period of 1,800 s (⊙) on the exit surface of M_4 (e).

temperature with the one experimentally measured. The temperature photos of the exit surface of M_4, using a thermal imager at 50, 200, 1,400, and 1,800 s, respectively, are shown in Fig. 8 a–d. Figure 8 e indicates the experimental values and the calculated ones during a 11 kW laser beam combining period of 1,800 s. One can see that the calculated results based on the model above established are basically consistent with the measurement.

6. Conclusions

In conclusion, we introduced a 19×1 laser incoherent space beam combiner with a laser combining power of 11 kW. To verify whether the beam combiner has good reliability in the long-term laser combining process, the finite element method was used to analyze the thermal–mechanical performances of all optical elements in the beam combiner. The multi-beam laser volumetric heat source model was established based on the overall heat source distribution of 19 laser beams of about 972 nm synchronously transmitted through optical elements. We concluded that the maximum temperature was distributed in the element with the largest central thickness, and the temperature of all optical elements tends to be stable after 1,400 s, which was still significantly lower than the softening point of fused silica material of 1,900 K. The maximum aperture number corresponding to the maximum thermal deformation was much smaller than the element processing tolerance of an aperture number of 1. The maximum stress of the optical elements in the combiner was less than the yield stress of fused silica of 50 MPa. Consequently, the beam combiner with laser power beyond 11 kW did not cause thermal cracking of internal optical elements. In addition, we experimentally measured the temperature of the window element of the beam combiner; the result of the comparison between the measurement and the simulation value showed that the established model exhibited good reliability and accuracy. Our finite element thermal method used

for the optical elements based on multi-beam laser volumetric heat source model and the experimental measurement proposed will be an effective reference for the evaluation of the safety and reliability of ultra-high power laser space combining system.

Acknowledgments

This work was supported by Serving Local Special Project of Shaanxi Provincial Department of Education, China under Grant No. 19JC040 and the Key Research and Development Projects in Shaanxi Province, China under Grant No. 2020GY-118.

References

1. M. John, P. R. Kalvala, M. Misra, et al., *Materials*, **14**, 3841 (2021).
2. D. Majumder, S. D. Chowdhury, and A. Pal, *IEEE J. Sel. Top. Quantum Electron.*, **27**, 0900409 (2021).
3. B. Y. Han, Y. W. Xu, K. B. Zhou, et al., *J. Russ. Laser Res.*, **42**, 598 (2021).
4. G. Q. Yang, L. S. Liu, Z. H. Jiang, et al., *Opt. Laser Technol.*, 101, 372 (2018).
5. Y. Bai, G. Z. Lei, H. W. Chen, et al., *IEEE Access*, **7**, 154457 (2019).
6. S. I. Derzhavin, V. P. Yakunin, R. V. Grishaev, et al., *J. Russ. Laser Res.*, **41**, 434 (2020).
7. J. Peñano, P. Sprangle, A. Ting, et al., *Opt. Soc. Am. B: Opt. Phys.*, **26**, 503 (2009).
8. H. B. Wang, Y. L. Song, Y. F. Yang, et al., *Opt. Express*, **28**, 33334 (2020).
9. M. Tian, D. Chu, Q. Yuan, et al., *Opt. Laser Technol.*, **139**, 106952 (2021).
10. B. C. Davis, G. S. Glaesemann, and I. Reimanis, *J. Am. Ceram. Soc.*, **103**, 7135 (2020).
11. P. F. Pan, H. W. Song, Z. H. Yang, et al., *Silicon*, **13**, 3163 (2021).
12. Q. H. Zhou, L. F. Chen, and X. Y. Xu., *Opt. Commun.*, **284**, 4207 (2011).
13. H. Chen, H. J. Yang, X. F. Yu, et al., *Appl. Opt.*, **52**, 4370 (2013).
14. Y. Jiang, S. B. He, W. Liao, et al., *J. Non-Cryst. Solids*, **515**, 1 (2019).
15. J. Y. Natoli, L. Gallais, H. Akhouayri, et al., *Appl. Opt.*, **41**, 3156 (2002).
16. R. Brückner, *J. Non-Cryst. Solids*, **5**, 123 (1970).
17. R. N. Raman, M. J. Matthews, J. J. Adams, et al., *Opt. Express*, **18**, 15207 (2010).
18. V. N. Mahajan and E. Acosta, *Appl. Opt.*, **59**, 120 (2020).
19. D. J. Brady and N. Hagen, *Opt. Express*, **17**, 10659 (2009).
20. C. A. Klein, *Opt. Eng.*, **48**, 113401 (2009).